Nuclear Instruments and Methods in Physics Research B 339 (2014) 1–7

Contents lists available at ScienceDirect

Nuclear Instruments and Methods in Physics Research B

journal homepage: www.elsevier.com/locate/nimb

Improved calculation of displacements per atom cross section in solids by gamma and electron irradiation

Ibrahin Piñera [a,*], Carlos M. Cruz [a], Antonio Leyva [a], Yamiel Abreu [a], Ana E. Cabal [a], Piet Van Espen [b], Nick Van Remortel [b]

[a] Centro de Aplicaciones Tecnológicas y Desarrollo Nuclear, CEADEN, 30 St. 502, Playa 11300, Havana, Cuba
[b] University of Antwerp, CGB, Groenenborgerlaan 171, 2020 Antwerpen, Belgium

ARTICLE INFO

Article history:
Received 4 August 2014
Received in revised form 26 August 2014
Accepted 27 August 2014
Available online 15 September 2014

Keywords:
Displacement per atom
Dpa cross section
Electron
Gamma
Monte Carlo simulation

ABSTRACT

Several authors had estimated the displacements per atom cross sections under different approximations and models, including most of the main gamma- and electron-material interaction processes. These previous works used numerical approximation formulas which are applicable for limited energy ranges. We proposed the Monte Carlo assisted Classical Method (MCCM), which relates the established theories about atom displacements to the electron and positron secondary fluence distributions calculated from the Monte Carlo simulation. In this study the MCCM procedure is adapted in order to estimate the displacements per atom cross sections for gamma and electron irradiation. The results obtained through this procedure are compared with previous theoretical calculations. An improvement in about 10–90% for the gamma irradiation induced dpa cross section is observed in our results on regard to the previous evaluations for the studied incident energies. On the other hand, the dpa cross section values produced by irradiation with electrons are improved by our calculations in about 5–50% when compared with the theoretical approximations. When thin samples are irradiated with electrons, more precise results are obtained through the MCCM (in about 20–70%) with respect to the previous studies.

1. Introduction

The issue of damage caused by different radiation sources in different materials has been and is still widely discussed by the scientific community. This topic is of great importance involving the changes they may induce in the properties of those materials. The primary event and one of the most important processes related with this radiation damage is the production of atom displacements, which first step is the generation of a primary knock-on atom (PKA), with kinetic energy T. If this interaction can be described through a differential cross section $d\sigma(E,T)/dT$, then for an incident radiation with energy E, which fluence is $\Phi(E)$, the total number of primary atoms per unit volume is:

$$N_T = N_a \int_{T_d}^{T_{\max}} \int_{E_c}^{E_{\max}} \frac{d\sigma(E,T)}{dT} \Phi(E)\, dE\, dT, \tag{1}$$

where N_a is the number of atoms per unit volume, T_d is the minimum energy an atom needs to be displaced, $T_{\max}$ is the maximum energy of the recoil atoms, E_c is the lowest radiation energy which can transfer energy T_d to a lattice atom and $E_{\max}$ is the maximum energy of the radiation spectrum.

Thus, for a monoenergetic incident fluence, it is possible to evaluate the total number of primaries per unit volume as:

$$N_T = N_a \Phi_0 \sigma(E_0, T_d), \tag{2}$$

being E_0 the energy of the incident radiation fluence Φ_0 and $\sigma(E_0, T_d)$ could be seen as the total atom displacement cross section. Therefore, the point is to find the adequate cross section for each case under study. However, there are no tools or methods for an accurate determination of such cross section for atom displacements determination in the case of electron and gamma irradiation at present.

In the late 1950's Oen and Holmes [1] and Cahn [2] proposed a methodology to calculate the atom displacements cross section in solids produced by gamma rays. In the last two decades several updated procedures for atom displacements cross section estimations have been proposed [3–7]. However, all those calculations have a restricted character and meaning, as will discussed in next section.

In a previous work [8] we presented an alternative approach to calculate the atom displacements distributions in high

* Corresponding author. Tel.: +53 7 2066109; fax: +53 7 2031220.
E-mail address: ipinera@ceaden.edu.cu (I. Piñera).

http://dx.doi.org/10.1016/j.nimb.2014.08.020
0168-583X/

temperature superconductors involving gamma radiation interactions and transport properties. Later, the contribution from positrons was also included in these studies [9], introducing a calculation procedure for atom displacements estimations [10].

Within this framework, this manuscript presents an improved methodology for the calculation of atom displacements cross section in solids by gamma rays and electrons irradiation. The results from previous mentioned theoretical calculations are then compared and analyzed with those obtained with our proposal.

2. Previous calculation procedures

Gamma radiation produces atom displacements through secondary electrons and positrons. The calculation of the differential cross section is thus complex, since involves different intermediate processes. Each of these processes may be dominant for a given energy and a given target material. Oen and Holmes [1] proposed a methodology to calculate displacement cross sections in solids by gamma rays. Cahn [2] also applied this methodology to calculate the total number of displaced atoms in germanium and silicon due to electrons and gamma rays of energies up to 7 MeV.

Following their idea, the true cross section in this case may be expressed formally by adding up all gamma-material interaction cross sections for the various mechanisms for energy transfer from primary gamma radiation to secondary electrons. For these processes, the intermediate electron behavior details in the lattice must be considered. Since one of the principal experimental advantages of gamma rays is near uniformity of damage production over large samples, it is felt that the most useful calculation considers the entire range of the electron as falling within the specimen. Thus, one additional result is the "thick target" cross sections for atom displacement by electrons.

Therefore, it is assumed that the energetic electrons produced by the gamma rays are stopped inside the solid sample. The average number of displaced atoms produced by an electron over its path, $\overline{n}(E_0)$, is thus found by integrating the elastic electron–atom interaction cross section over the electron range, also known as the displacements cross section $\sigma_d(E)$, obtaining:

$$\overline{n}(E_0) = N_a \int_0^{E_0} \frac{\sigma_d(E)}{(-\mathrm{d}E/\mathrm{d}x)}\, dE, \tag{3}$$

where $(-\mathrm{d}E/\mathrm{d}x)$ represents the electron energy change with respect to the electron path [11]. The elastic electron–atom interaction cross section is discussed in details in the next section.

For the gamma-material interaction cross sections Oen and Holmes considered Compton scattering with the assumption of single displacement for the primary recoiled atom. Cahn considers the main three processes of gamma interaction with matter producing secondary electrons: Compton scattering, photoeffect and pair production. In the last two decades several updated cross sections have been proposed.

The calculation by Baumann [3] was based on Oen's electron-induced displacement cross section [12] with the displacement energies of 28 eV and 40 eV, considering Compton scattering and pair production. Alexander and Rehn [13] carried out their calculation considering all three gamma-material interactions with the McKinley–Feshbach approximation for electron-induced displacement [14]. Kwon and Motta [5] proposed atom displacements cross sections for various metals, considering three gamma-material interactions and using Oen's electron-induced displacement cross section with the displacement energies of 24 eV and 40 eV. The contribution of positrons produced from the pair production was neglected in Kwon–Motta's calculation and was treated as electrons's in Baumann's and Alexander–Rehn's calculations.

Fukuya and Kimura [7] calculated gamma-induced atom displacements cross sections of iron considering all three gamma-material interactions with the McKinley–Feshbach approximation for electron-induced displacement and displacement energies of 25 eV and 40 eV. They took into account both electron and positron-induced displacements by separate.

All these calculations have a restricted character. They follow the Oen–Holmes–Cahn calculation procedure, which does not take into account the cascade process of the showering of gamma rays and the secondary electron and positron, occurring during radiation transport inside materials. They neither can obtain the volume distribution of atom displacements damage inside the material.

3. The Monte Carlo assisted Classical Method

The proposed Monte Carlo assisted Classical Method (MCCM) relates the Oen–Holmes and Cahn established theories [1,2] (here on referred as "classical theories") about atom displacements to the electron and positron fluence distributions calculated from the Monte Carlo simulation.

The proposal mainly consists in replacing the analytical distributions of particles produced in gamma and electron interactions with material by those obtained through the Monte Carlo simulation of radiation transport in matter. That is, defining the total number of atom displacements (AD) per volume unit as:

$$N_{\mathrm{AD}} = \frac{1}{V} \int_0^{E_0} \overline{n}(E) N_e(E)\, dE, \tag{4}$$

where V is the studied volume, $\overline{n}(E)$ is given by Eq. (3), and $N_e(E)$ is the energy distribution of secondary particles calculated by Monte Carlo simulation in the volume V. The code system used for simulation purposes (described in Section 3.2) allows to obtain the average energy fluence distribution, $\Phi_e(E)$, in the volume of the studied material. In order to study the in-depth and volumetric AD distributions, it is possible to divide the volume of the material in subvolumes (voxels). In this way the energy fluence distribution in each one of these voxels can be obtained. Thus, the energy distribution of secondary particles can be computed as $\Phi_e(E) \times S$, being S the total section of the material (or voxel) surrounding the volume V.

It is known that the displacement of an atom occurs for particle energies higher than a certain cutoff energy E_c, corresponding to the threshold displacement energy of the target atom, T_d. On the other hand, all the simulation results are obtained normalized per incident photon or particle source. Thus, knowing the source fluence used in an specific study, it is possible to obtain the total number of AD, rewritten (4) after making some transformation:

$$N_{\mathrm{AD}} = N_a \Phi_0 S \int_{E_c}^{E_0} \sigma_d^*(E) \Phi_e(E)\, dE, \tag{5}$$

with

$$\sigma_d^*(E) = \frac{S}{V} \int_{E_c}^{E} \frac{\sigma_d(E')}{(-\mathrm{d}E'/\mathrm{d}x)}\, dE', \tag{6}$$

where the displacement cross section, $\sigma_d(E)$, is discussed in the next section.

A more common used way of expressing atom displacements is through the displacements per atom (dpa) magnitude, which can be obtained normalizing to the total number of atoms, N_{AD}/N_a. Furthermore, for compound materials all the constituent atomic species could be considered taking into account the relative fraction n_k of the k-atom in its crystalline sublattice. Thus the total displacements per atom can be calculated as the sum over all the atomic species:

$$N_{dpa} = \sum_k \left(n_k \Phi_0 S \int_{E_c^k}^{E_0} \sigma_d^{*k}(E) \Phi_e(E)\, dE \right). \quad (7)$$

The electron or positron cutoff kinetic energy (E_c^k) depends on the k-atom mass, M_k, and displacement energy, T_d^k:

$$E_c^k = \sqrt{(mc^2)^2 + \frac{M_k c^2}{2} T_d^k} - mc^2. \quad (8)$$

Expression (7) can be rewritten in the form of (2):

$$N_{dpa}^k = \Phi_0\, \sigma_{dpa}^k(E_0, T_d^k), \quad (9)$$

by defining the effective dpa cross section for the k-atom, depending on the incident radiation energy and the displacement energy, as follows:

$$\sigma_{dpa}^k(E_0, T_d^k) = n_k S \int_{E_c^k}^{E_0} \sigma_d^{*k}(E) \Phi_e(E)\, dE. \quad (10)$$

In this way, the MCCM constitutes a substantial improvement to the Oen–Holmes and Cahn algorithms, and it is not a simple quiddity. It adapts these algorithms to the modern calculations of the gamma and electron radiation transport through Monte Carlo method. In this case the approximate expressions taken *a priori* for the electron energy distributions in their primary interactions are not used, like it was made, for example, by Belevtsev and coworkers [6].

The fact of introducing $\Phi_e(E)$ allows to take into account more realistic electron and positron energetic distributions in any point of the solid matrix. In addition, it is possible to obtained for the first time the in-depth dpa distribution profiles subdividing the material volume in smaller sub-volumes for the simulation. MCCM procedure also permits to evaluate more accurately the contribution to dpa from different crystalline sublattices depending on the incident gamma or electron radiation.

3.1. Displacements cross section

The different physical assumptions mentioned in previous chapter result in differences in the size and energy dependence of the displacement cross section. In order to get an analytical expression, the α^2 approximation of McKinley and Feshbach [14] is used for primary knock-on atom formation. It is possible to integrate the McKinley–Feshbach differential cross section obtaining:

$$\sigma_{PKA}^k(E) = \sigma_0(E) \times \left\{ 2\tau - 1 - \beta^2 \ln(2\tau) \pm \pi\alpha\beta \left[2\sqrt{2\tau} - \ln(2\tau) - 2 \right] \right\}, \quad (11)$$

where $\sigma_0(E) = \pi r_0^2 Z_k^2 / \beta^4 \gamma^2$ with Z_k being the atomic number of the k-atom, r_0 is the electron classic radius, β is the electron to light velocity ratio, $\gamma^2 = 1/(1-\beta^2)$, α is the fine-structure factor ($\cong Z_k/137$) and $\tau = T_{\max}^k / 2T_d^k$, being $T_{\max}^k$ the maximum kinetic energy of the corresponding recoil atom. This cross section includes the positron–atom scattering through the term involving $\pi\alpha\beta$, which takes a positive (negative) sign for electrons (positrons).

On the other hand, introducing the damage function allows to include the atom displacement cascade phenomenon for higher atom recoil energies. The Kinchin–Pease model [15] is used for the damage function in order to obtain an analytical cross section integrating this expression. Thus, the integration now gives the total displacement cross section including cascade processes ($T^k \geqslant 2T_d^k$):

$$\sigma_d^k(E) = \sigma_0(E) \times \left\{ \tau(1-\beta^2) + \tau \ln(\tau) + C_1 \beta^2 \pm \pi\alpha\beta \left(\tau - C_2\sqrt{\tau} + C_1 \right) \right\}, \quad (12)$$

where $C_1 = (1 - \ln 2) \approx 0.307$ and $C_2 = 2(2 - \sqrt{2}) \approx 1.172$. This expression applies then for $E \geqslant E_c^k(2T_d^k)$. This is the threshold electron (positron) kinetic energy when displacement cascades start occurring.

3.2. Description of the simulation process

For the simulations performed within the MCCM, the general-purpose Monte Carlo code MCNPX version 2.6b [16] is used. This code was considered since it gives directly the fluence distribution for electrons and positrons corresponding to a given energy interval, for the flux averaged over a cell. The simulation involves all the physical processes taking place in matter when either gamma rays or electrons pass through it. As mentioned before, in order to study the in-depth and volumetric dpa distributions, the volume of the material is divided in voxels and the energy fluence distribution is obtained in each one of these voxels.

The sample geometry is defined in each case under study. In order to fulfill with the "thick layer" condition related with expression (3), the chosen sample dimensions are selected in correspondence to the secondary electron range values for the selected incident energies. Even so, it should be expected an overestimation since not all the higher energy electrons will deposit its energy inside the voxel in which they are created.

The irradiation process is simulated with a large number of incident particles impacting on one of the sample surfaces. In all cases, the results are normalized to the total number of histories (incident photons or electrons and their secondary particles).

4. Comparing MCCM with the previous calculations

Oen and Holmes calculate the cross sections for the displacement of lattice atoms by gamma rays up to 5 MeV energies [1]. They analyzed different gamma interaction processes with matter leading to secondary electron generation. The principal contribution is found to come from the Compton effect, when the atoms are displaced by the gamma rays produced electrons. Several authors had estimated the dpa cross sections under different approximations and models, including most of the gamma-material interaction processes [2–7]. The common conclusion is that the main contribution to dpa cross section comes from the Compton effect for lighter and medium elements and for energies up to about 10 MeV.

On the other hand, no exact analytical formula covering the whole energy range is available for the differential cross section for producing an electron or a positron in the cases of photoelectric effect and pair production processes. The previous works used numerical approximation formulas which are applicable for limited energy ranges. For this reason, is usual to use the Klein–Nishina analytical expression for Compton effect [17] to perform dpa calculations.

4.1. Secondary particle fluence distribution

First, some analysis concerning the calculated energy fluence distributions from the Monte Carlo simulation are presented. For the calculations the material and experimental conditions used by Belevtsev and coworkers in [6] are employed. They used the theoretical Compton electrons distribution to estimate the dpa cross section in $YBa_2Cu_3O_7$ (YBCO) superconducting material by gamma irradiation with ^{60}Co source.

In the case of MCCM, the fluence energy distributions are obtained from the Monte Carlo simulation of radiation transport through matter by means of the MCNPX code [16]. This distribution is calculated for gamma incident energy of 1.25 MeV

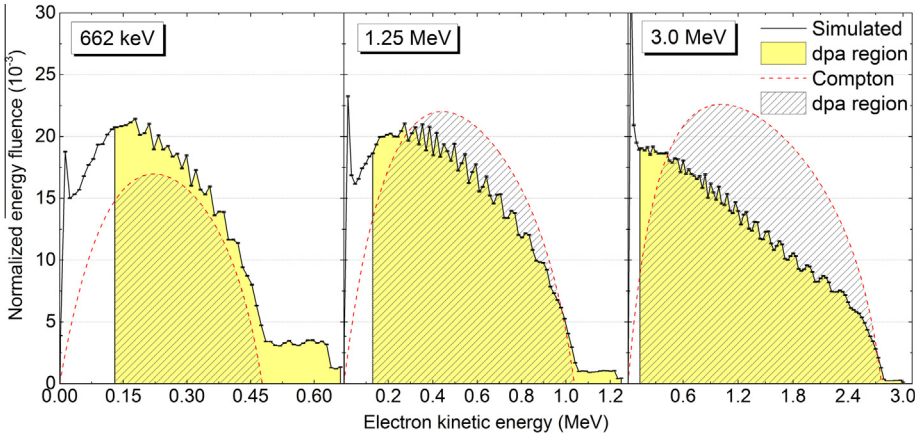

Fig. 1. Energy fluence distributions obtained by Monte Carlo simulation inside the sample (continuous black lines). The theoretical distribution of Compton electrons is also included (dashed red curves). Filled and stripy regions correspond to the dpa integration interval ($E_c^k \rightarrow E_{max}$) for simulated and Compton distributions respectively. All values are normalized to the incident corresponding fluence. (For interpretation of the references to colour in this figure legend, the reader is referred to the web version of this article.)

(^{60}Co averaged energy). Fluence distributions for incident gamma energies below (662 keV from ^{137}Cs source) and above (3 MeV) are also computed. Fig. 1 shows these results, where all fluence values are normalized to the incident corresponding one.

An interesting fact is related to the shape of these distributions. First, the ejected photoelectrons can obtain the highest kinetic energy values (close to E_0) with an appreciable relative intensity for lower incident energies, which may give an important contribution to dpa values. In addition, the continuous electron contribution arising from Compton scattering, as well as from the relaxation processes, becomes a broader single-mode distribution when increasing E_0 values, with a width near to the maximum Compton electrons kinetic energy.

The dashed curves in Fig. 1 represent the calculated distribution of Compton electrons fluence following the Klein–Nishina analytical expression. These values are also normalized to incident gamma fluence for better comparison. The filled region below the simulated distribution indicates the fluence of particles that contribute to the formation of oxygen displacements in the YBCO material ($E_c^k \approx$130 keV). This is the region that is integrated in Eq. (7) to calculate dpa values. The stripy region means the same, but for the analytical Compton distribution. It is easy to note the difference between simulated and analytical distributions, corresponding to the primary Compton part of the fluence spectrum.

For the gamma energy at 662 keV an underestimation of the theoretical effective fluence compared to the simulated one is observed (about 69%). In this case the contribution of the calculated Compton distribution to dpa formation is about 76% of the corresponding simulated one. For lower gamma energy the contribution from Compton electrons to the generated effective fluence inside the material is smaller (i.e. for 122 keV is only about 4%). For incident photons with 1.25 MeV energy a better agreement between the Compton part of the spectrum with the simulated one is observed. In this case the analytical distribution overestimates the simulated one with about 6%. The contribution to dpa formation from Compton is about 9% higher relative to the simulated one for this energy.

For higher incident energy more photons and secondary particles will escape from the sample, since the mean free path for photons and electron's ranges are higher. For example, the mean free path for photons with 1.25 MeV is about 4 cm (electron range about 1.5 mm) and about 24% of the primary does not interact with the target sample, which is 2.2 cm width in this calculations, like in the reference work [6]. In this case, not all photons from the source will interact inside the sample and neither do all the produced secondary electrons. The Compton energy range of the fluence spectrum will be wider for higher gamma energies, since $E_{max} \approx E_0$. However, pair production interaction processes will appear and increase in importance with increasing gamma energy. For 3 MeV incident gamma energy the contribution from the primary Compton electron part is also higher than the simulated one by about 33%, contributing with more than 43% to the dpa calculation.

4.2. Dpa induced by gamma irradiation

Taking the previous works reported on the estimation of the dpa cross sections for gamma induced displacements in some materials as a reference, the MCCM procedure is applied and both results are compared. It is good to clarify that all the simulations for this comparisons were performed for large material dimensions (3 cm × 3 cm × 3 cm). In this way it is ensured that the maximum number of photons and electrons interact inside the material. It minimizes the underestimation from our calculations due to small material sample sizes. The key for all those previous "classical" estimations is to assume that the electrons are stopped inside the solid sample. In addition, positrons are considered as electrons in these calculations, as was done in all previous estimations, with exception of Cahn [2] and Fukuya and Kimura [7]. Despite all this, in general, one can expect an overestimation from these "classical" approaches, since they are based on analytical and numerical distributions for the gamma-material interaction processes on infinite media, considering that all primary photons interact with the target material.

We start with the former work from Oen and Holmes [1]. They presented the calculation of the dpa cross section by gamma rays through the Compton process as function of the incident gamma energy for some elements with different displacement energies. The corresponding dpa cross sections for Cu through MCCM for two displacement energies are presented in Fig. 2 together with their results for better comparison. A relative good agreement is seen between our calculations and those from Oen and Holmes. As expected, there is an overestimation from their results for lower energies. Their results are higher in about 10–40% than ours for incident gamma energies up to 2.5 MeV in the case of $T_d = 15$ eV and 10–90% in the case of $T_d = 25$ eV. For energies higher than 3 MeV their underestimation is consequence of considering only the Compton processes, and it is known that for higher energies

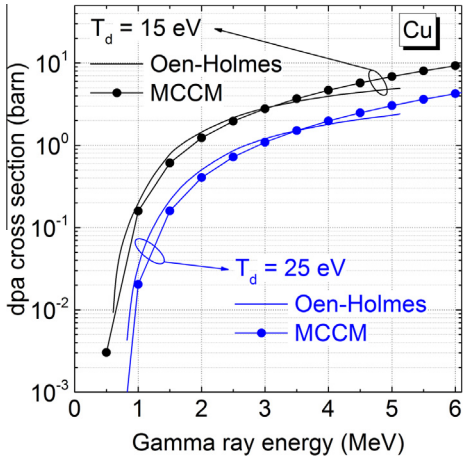

Fig. 2. Dpa cross sections calculated by Oen and Holmes [1] and MCCM in Cu for two values of the displacement energy.

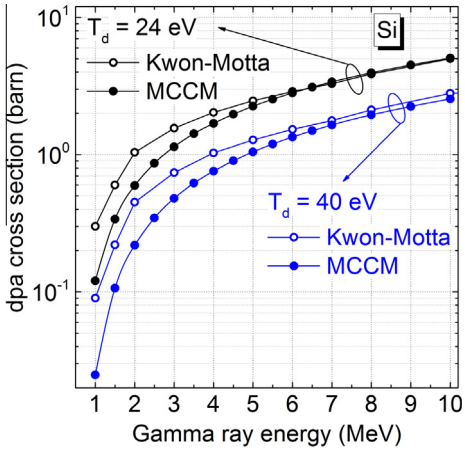

Fig. 4. Dpa cross sections in Si according to Kwon and Motta [5] and MCCM for two values of the displacement energy.

the pair production process increases its importance [7]. Also, they do not included in their calculations the atom displacements cascade phenomena that becomes important at higher energies.

Cahn also applied the same procedure to estimate the dpa cross sections in Si and Ge under gamma irradiation up to 7 MeV [2]. He included the three main gamma-material interaction processes and the cascade phenomenon in his calculations. Our results through MCCM and Cahn's are presented in Fig. 3 for Si using two values of the displacement energy. An overestimation in his calculations is noted, being about 1.1–1.4 times our results for $T_d = 15$ eV. For $T_d = 30$ eV that difference is a bit higher, about 1.2–1.9 times. It is then found that this overestimation decreases for higher incident gamma energies and for lower displacement energies.

Something different happens with the results of Kwon and Motta [5]. Their results for Si and the corresponding ones from MCCM are presented in Fig. 4. Their calculations overestimate ours with factors 1.1–2.5 ($T_d = 24$ eV) and 1.2–3.6 ($T_d = 40$ eV) times up to 5 MeV incident gamma energy. For higher gamma energies Kwon–Motta's cross section shows a more gentle energy dependence, with a difference of only 2% ($T_d = 24$ eV) and 9% ($T_d = 40$ eV) relative to ours for 10 MeV incident energy. Such gentle energy dependence is probably because the displacements by positrons was neglected in their calculations.

Some other estimations of dpa cross sections have been done in Fe by several authors. Fig. 5 shows those results for different displacement energies and approximations, together with our results through MCCM for 25 eV and 40 eV atom displacement energies for comparison. All those authors considered photo-electric effect, Compton and pair production processes in the calculation of the dpa cross sections. The Kwon and Motta calculations were discussed above and similar comments apply for Fe. Higher difference for lower energies is obtained (1.5–7.6 times) since they used $T_d = 24$ eV and our calculations in this case are based on $T_d = 25$ eV. The estimations by Fukuya and Kimura [7], using the Kinchin–Pease model for the damage function, are 1.2–1.5 times higher than ours. They considered both electrons and positrons, concluding that it results in a reduction by a factor of 1.1 compared to an approximation treating a positron as an electron, as considered in our calculations.

For the case of $T_d = 40$ eV, the calculations by Baumann [3] gave higher dpa cross sections by a factor of 1.4–2.6 than the present calculation. He used Oen's tabulated electron-induced cross sections [12]. The difference with the results by Alexander [4] is smaller, just about 1.2–1.3 higher than MCCM calculations. He used the same differential PKA cross section (McKinley–Feshbach approximation), but using the Norgett–Robinson–Torrens (NRT) model [18] for the damage function. Fukuya and Kimura concluded

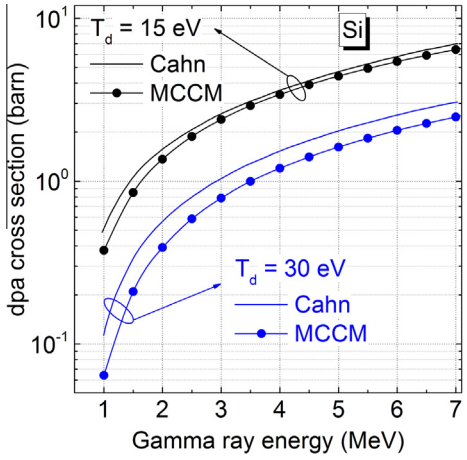

Fig. 3. Dpa cross sections in Si estimated by Cahn [2] and calculated by MCCM for two values of the displacement energy.

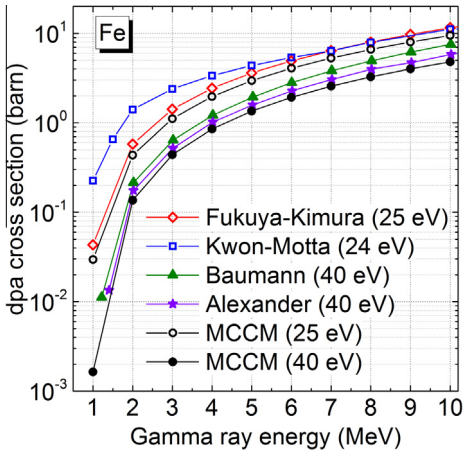

Fig. 5. Dpa cross sections in Fe by Fukuya and Kimura [7], Kwon and Motta [5], Baumann [3], Alexander [4] and MCCM.

that the NRT model gave results that are 1.3 times smaller than the Kinchin–Pease model for Fe [7].

4.3. Dpa induced by electron irradiation

Oen and Holmes [1] and Cahn [2] also calculated the number of displacements per incident electron in some metals for different displacement energies through the formula (3). In order to compare with their results the expression (5), normalized per incident electrons, is used.

Simulations for different incident electrons energies are then performed, considering large material dimensions, to ensure that most of the incident electrons interact inside the material. In this way the results will be consequent with the "thick target" approximation assumed in the formula (3) in order to have a fair comparison.

Their results and those through MCCM for Cu and Si and displacement energies used in previous mentioned works are presented in Figs. 6 and 7. A good qualitative agreement between our calculations and those from Oen and Holmes is found. MCCM calculations are about 2–6% higher than their estimations for electron energies about 1 MeV. For higher electron energies, the difference increases up to 50% in the case of $T_d = 15$ eV and ~40% for $T_d = 25$ eV for electron energies about 5 MeV. The

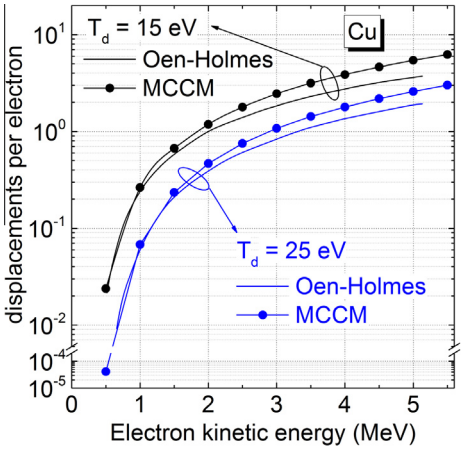

Fig. 6. Number of displacements per electron calculated by Oen and Holmes [1] and MCCM in Cu for two values of T_d.

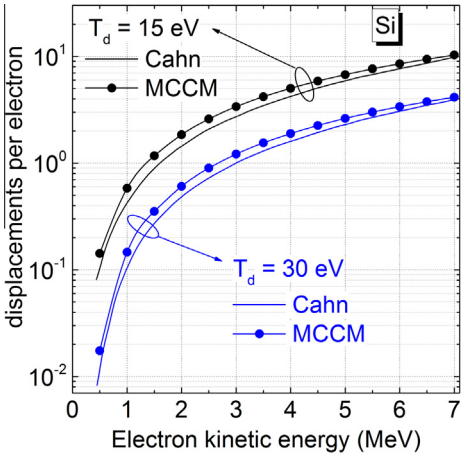

Fig. 7. Number of displacements per electron in Si estimated by Cahn [2] and calculated by MCCM for two values of T_d.

underestimation of their results is related to the fact that their calculations considered displacements induced by an electron along its path in the material, but they do not take into account the secondary particles produced in the electron-material interaction processes. On the contrary, all those processes are included in the Monte Carlo simulation performed in the framework of MCCM. Also, for higher energies their underestimation is consequence of ignoring the atom displacements cascade phenomenon.

Cahn's results also show a general qualitative agreement with MCCM for all electron and displacement energies, with an underestimation in his calculations that decreases for higher electron energies, being about 5–36% relative to our results in the studied energy range. This underestimation is up to 5% lower for $T_d = 30$ eV than for $T_d = 15$ eV. For higher electron energies, near 7 MeV, Cahn's underestimation is only a factor 1.1 times below our results. This could be a consequence of the approximation used by Cahn for the stopping power evaluation. He used empirical range-energy formulas [19], which present different energy-dependence for higher energies than the one used in MCNPX and MCCM.

The MCCM results are now compared with some other previous estimations of dpa induced by electron irradiation in thin samples. All these studies estimated displacements per atom values as the product of the Oen's cross section [12] and the fluence used for irradiation. In these cases, the results are overestimated as consequence of the Oen's "thick target" approximation, which assumes that all the electrons come to rest within the solid sample.

Starting with the work by Basu et al. [20] on electron-beam-irradiation effects in bulk YBCO. They studied irradiation effects in a transmission electron microscope using 100–300 keV electrons. Basu et al. analyzed thin foils of YBCO in form of 30 μm thick slabs. The energies they used lead to electron ranges of about 45 to 250 μm. Their experiments are simulated and the dpa values through MCCM are calculated (with $T_d = 18$ eV). Results are presented in Table 1. Their results are 1.2–1.4 times higher than our calculations for energies 200–300 keV, being 3.2 times higher for lower energies of 150 keV. Then, our results improve theirs in about 20–69% for the studied electron energies.

Giapintzakis and coworkers used 350 keV electrons to study point defects in YBCO single crystals [21]. They calculated dpa values in a way similar to that previously explained, using $T_d = 20$ eV and different electron fluences, obtaining 2.05×10^{-4} and 8.19×10^{-4} dpa. Their sample is even thinner, with 9 μm width, and electrons with 350 keV energy have about 318 μm of range in YBCO. Their experiment is also simulated and the dpa values for both fluences in the sample are calculated, resulting in 1.30×10^{-4} and 5.20×10^{-4} dpa respectively, values about 1.6 times lower than their estimations. Then, MCCM improves the results in this case in ~37%.

Table 1
Electron-irradiation (with energy E_0) induced dpa values estimated in previous works and those calculated through MCCM. The relative difference between them, (dpa[Ref.]-dpa[MCCM])/dpa[Ref.], is also showed.

Refs.	E_0 (MeV)	dpa		Rel. dif. (%)
		in Ref.	MCCM	
[20]	0.15	1.51	0.47	69
	0.20	2.10	1.50	29
	0.25	2.99	2.40	20
	0.30	3.38	2.68	21
		3.76	2.99	20
[21]	0.35	2.05×10^{-4}	1.30×10^{-4}	37
		8.19×10^{-4}	5.20×10^{-4}	37
[22]	2.50	5.00×10^{-4}	2.36×10^{-4}	53
		1.00×10^{-3}	5.07×10^{-4}	49

Another study in which the authors tried to evaluate dpa induced by higher energy electrons (2.5 MeV) is the one carried out by Yacoby and his group [22]. They investigated the effect of two doses of 2.5 MeV electron irradiation on the irreversibility line of a ceramic YBCO sample. They also estimated dpa values using Oen's cross sections for $T_d = 20$ eV for all atoms in the material. Their sample is 100 μm width, but electrons with 2.5 MeV have penetration higher than 3 mm. Their experiment is simulated and the corresponding dpa values are calculated. The results through MCCM are 2.0–2.1 times lower than their estimations (Table 1). In this case, the improvements in our results are about 53% and 49%.

5. Conclusions

The previously proposed Monte Carlo assisted Classical Method was used in order to calculate the displacements per atom cross sections for gamma and electron irradiation. The MCCM results were compared with previous theoretical calculations. The main difference is related to the secondary particle spectra considered for calculations, which depends on the incident radiation nature and on its interaction processes with the material. The difference between the calculated analytical distributions and the simulated ones is remarkable. The simulation process gives a more realistic approach by taking into account the material dimensions and all interaction and transport processes of photons and electrons/positrons in matter.

A relative qualitative agreement between our calculations and those from Oen–Holmes and Cahn methodologies was observed for the analyzed electron and atom displacement energies. An improvement in about 10–90% for the gamma irradiation induced dpa cross section was observed in our results on regard to the previous evaluations for the studied incident energies. On the other hand, the dpa cross section values produced by irradiation with electrons were improved by our calculations in about 5–50% when compared with the "classical" approximations. When thin samples were irradiated with electrons, more precise results were obtained through the MCCM (in about 20–70%) with respect to the previous studies.

Therefore, the complex behavior of the gamma and electron interaction processes with matter can not be neglected at all for dpa calculations. The MCCM methodology supports the introduction of a more realistic treatment for gamma and secondary electron/positron transport as demonstrated here with Monte Carlo based simulations.

Acknowledgments

This study was possible thanks to the collaboration agreement between the University of Antwerp in Belgium, the Higher Institute of Technology and Applied Sciences and the Center of Technological Applications and Nuclear Developments in Cuba. We also acknowledge to the Nuclear Energy and Advanced Technologies Agency of the Ministry of Science, Technology and Environment of Cuba by the support of this study through the project PRN/6-2/3.

References

[1] O.S. Oen, D.K. Holmes, Cross sections for atomic displacements in solids by gamma rays, J. Appl. Phys. 30 (8) (1959) 1289–1295, http://dx.doi.org/10.1063/1.1735307.
[2] J.H. Cahn, Irradiation damage in germanium and silicon due to electrons and gamma rays, J. Appl. Phys. 30 (8) (1959) 1310–1316, http://dx.doi.org/10.1063/1.1735310.
[3] N.P. Baumann, Gamma-ray induced displacement in D20 reactors, in: G. Tsotridis, R. Dierckx, P. D'Hondt (Eds.), 7th ASTM-EURATOM Symposium on Reactor Dosimetry, Kluwer, Dordrecht, The Netherlands, 1992, p. 689.
[4] D.E. Alexander, Defect production considerations for gamma ray irradiation of reactor pressure vessel steels, J. Nucl. Mater. 240 (1997) 196–204, http://dx.doi.org/10.1016/S0022-3115(96)00713-1.
[5] J. Kwon, A.T. Motta, Gamma displacement cross-sections in various materials, Ann. Nucl. Energy 27 (18) (2000) 1627–1642, http://dx.doi.org/10.1016/S0306-4549(00)00024-4.
[6] B.I. Belevtsev, I.V. Volchok, N.D. Dalakova, V.I. Dotsenko, L.G. Ivanchenko, A.V. Kuznichenko, I.I. Lagvinov, Effect of γ-irradiation on superconductivity in polycrystalline $YBa_2Cu_3O_{7-\delta}$, Phys. Status Solidi (a) 181 (2000) 437, http://dx.doi.org/10.1002/1521-396X(200010)181:2437::AID-PSSA4373.0.CO;2-L.
[7] K. Fukuya, I. Kimura, Calculation of gamma induced displacement cross-sections of iron considering positron contribution and using standard damage model, J. Nucl. Sci. Technol. 40 (6) (2003) 423–428, http://dx.doi.org/10.1080/18811248.2003.9715375.
[8] I. Piñera, C.M. Cruz, Y. Abreu, A. Leyva, Determination of atom displacement distribution in ybco superconductors induced by gamma radiation, Phys. Status Solidi (a) 204 (7) (2007) 2279–2286, http://dx.doi.org/10.1002/pssa.200622155.
[9] I. Piñera, C. Cruz, Y. Abreu, A. Leyva, Monte carlo simulation study of the positron contribution to displacements per atom production in ybco superconductors, Nucl. Instrum. Methods B 266 (22) (2008) 4899–4902, http://dx.doi.org/10.1016/j.nimb.2008.08.002.
[10] I. Piñera, C.M. Cruz, Y. Abreu, A. Leyva, A.E. Cabal, P.V. Espen, Monte Carlo assisted classical method for the calculation of dpa distributions in solid materials, in: Nuclear Science Symposium Conference Record, NSS'08, IEEE, 2008, 2008, pp. 2557–2560, http://dx.doi.org/10.1109/NSSMIC.2008.4774878.
[11] H.A. Bethe, J. Ashkin, Passage of radiation through matter, in: E. Segrè (Ed.), Experimental Nuclear Physics, vol. I, John Wiley & Sons Inc, New York, 1953, pp. 166–357.
[12] O.S. Oen, Cross sections for atomic displacements in solids by fast electrons, Oak Ridge National Laboratory Report No. ORNL-4897, 1973.
[13] D.E. Alexander, L.E. Rehn, Gamma-ray displacement damage in the pressure vessel of the advanced boiling water reactor, J. Nucl. Mater. 217 (1–2) (1994) 213–216, http://dx.doi.org/10.1016/0022-3115(94)90325-5.
[14] W.A. McKinley, H. Feshbach, The coulomb scattering of relativistic electrons by nuclei, Phys. Rev. 74 (12) (1948) 1759–1763, http://dx.doi.org/10.1103/PhysRev. 74.1759.
[15] G.H. Kinchin, R.S. Pease, The displacement of atoms in solids by radiation, Rep. Prog. Phys. 18 (1955) 1–51, http://dx.doi.org/10.1088/0034-4885/18/1/301.
[16] J.S. Hendricks, G.W. McKinney, H.R. Trellue, J.W. Durkee, J.P. Finch, M.L. Fensin, M.R. James, D.B. Pelowitz, L.S. Waters, F.X. Gallmeier, J.C. David, MCNPX™ Version 2.6.B, Los Alamos National Laboratory, Report LA-UR-06-3248, 2006.
[17] O. Klein, Y. Nishina, über die streuung von strahlung durch freie elektronen nach der neuen relativistischen quantendynamik von dirac, Z. Phys. 52 (11–12) (1929) 853–868, http://dx.doi.org/10.1007/BF01366453.
[18] M.J. Norgett, M.T. Robinson, I.M. Torrens, A proposed method of calculating displacement dose rates, Nucl. Eng. Des. 33 (1) (1975) 50–54, http://dx.doi.org/10.1016/0029-5493(75)90035-7.
[19] L. Katz, A.S. Penfold, Range-energy relations for electrons and the determination of beta-ray end-point energies by absorption, Rev. Mod. Phys. 24 (1) (1952) 28–44, http://dx.doi.org/10.1103/RevModPhys. 24.28.
[20] S.N. Basu, T.E. Mitchell, M. Nastasi, Electron-beam-irradiation effects in bulk $YBa_2Cu_3O_{7-X}$, J. Appl. Phys. 69 (5) (1991) 3167–3171, http://dx.doi.org/10.1063/1.348586.
[21] J. Giapintzakis, D.M. Ginsberg, M.A. Kirk, S. Ockers, Testing models of the symmetry of the superconducting pairing state by low-temperature electron irradiation of an untwinned single crystal of $YBa_2Cu_3O_{7-\delta}$, Phys. Rev. B 50 (21) (1994) 15967–15973, http://dx.doi.org/10.1103/PhysRevB.50.15967.
[22] E.R. Yacoby, A. Shaulov, Y. Yeshurun, M. Konczykowski, F. Rullier-Albenque, Irreversibility line in $YBa_2Cu_3O_7$ samples: a comparison between experimental techniques and effect of electron irradiation, Physica C 199 (1992) 15–22, http://dx.doi.org/10.1016/0921-4534(92)90534-J.